TÜBİTAK

Turkish Journal of Biology

http://journals.tubitak.gov.tr/biology/

Research Article

Turk J Biol
(2018) 42: 63-75

doi:10.3906/biy-1706-6

Ultrasound-enhanced gene delivery to alfalfa cells by hPAMAM dendrimer nanoparticles

Amin AMANI[1], Nasser ZARE[1,*], Asadollah ASADI[2], Rasool ASGHARI-ZAKARIA[1]

[1]Department of Agronomy and Plant Breeding, Faculty of Agriculture and Natural Resources, University of Mohaghegh Ardabili, Ardabil, Iran

[2]Department of Biology, Faculty of Basic Sciences, University of Mohaghegh Ardabili, Ardabil, Iran

Received: 01.06.2017 • **Accepted/Published Online:** 30.12.2017 • **Final Version:** 15.02.2018

Abstract: Cationic polyamidoamine (PAMAM) dendrimers are highly branched nanoparticles with unique molecular properties, which make them promising nanocarriers for gene delivery into cells. This research evaluated the ability of hyperbranched PAMAM (hPAMAM)-G2 with a diethylenetriamine core to interact with DNA, its protection from ultrasonic damage, and delivery to alfalfa cells. Additionally, the effects of ultrasound on the efficacy of hPAMAM-G2 for the delivery and expression of the *gus*A gene in the alfalfa cells were investigated. The electrophoresis retardation of plasmid DNA occurred at an N/P ratio (where N is the number of hPAMAM nitrogen atoms and P is the number of DNA phosphorus atoms) of 3 and above, and hPAMAM-G2 dendrimers completely immobilized the DNA at an N/P ratio of 4. The analysis of the DNA dissociated from the dendriplexes revealed a partial protection of the DNA from ultrasound damage at N/P ratios lower than 2, and with increasing N/P ratios, the DNA was better protected. Sonication of the alfalfa cells in the presence of ssDNA-FITC-hPAMAM increased the ssDNA delivery efficiency to 36%, which was significantly higher than that of ssDNA-FITC-hPAMAM without sonication. Additionally, the efficiency of transfection and the expression of the *gus*A gene were dependent on the N/P ratio and the highest efficiency (1.4%) was achieved at an N/P ratio of 10. The combination of 120 s of ultrasound and hPAMAM–DNA increased the *gus*A gene transfection and expression to 3.86%.

Key words: Gene transfer, hPAMAM–DNA complex, *Medicago sativa* L., polyamidoamine dendrimers, sonication

1. Introduction

Alfalfa is a perennial forage crop that is widely grown throughout the world (Smith et al., 2000). Moreover, it has been shown that alfalfa has healthcare effects, such as the reduction of glucose, cholesterol, and lipoprotein concentrations in plasma (Farsani et al., 2016). Genetic transformation of plants allows the introduction of a gene or genes into one species from an unrelated plant or nonplant species and thus plays an important role in the qualitative and quantitative improvement of crop products. Furthermore, genetic transformation of plants has great potential in the production of protein-based drugs and basic plant biology.

Reporter genes enable visual screening and identification of transgenic cells in a large background of nontransgenic cells and so provide a powerful tool for transient and stable genetic transformation studies. The *gus*A gene encoding the β-glucuronidase (GUS) enzyme is one the most effective, simple, reliable, and cost-effective reporter systems used for identification of genetically transformed plant cells in transgenic studies (Xiong et al., 2011). Several methods have been developed for the genetic transformation of plants: *Agrobacterium*-mediated transformation (Nanasato et al., 2013; Tohidifar et al., 2013), biolistic (Daniell et al., 1990; Altpeter et al., 2005), ultrasound (Joersbo and Brunstedt, 1990; Liu et al., 2006), protoplast transformation that includes electroporation and polyethylene glycol-mediated transformation (Park et al., 2015; Burris et al., 2016), and silicon carbide (Frame et al., 1994). The susceptibility of all plant species and tissues to *Agrobacterium* is not the same and the transformation efficiency of this method for monocotyledonous plants is still low and unsatisfactory (Naqvi et al., 2012). The main disadvantages of biolistics (particle bombardment) include the high cost of biolistics devices and accessories, and the integration of multiple copies of the transgene in the plant genome (Finer et al., 1992). Protoplasts are plant cells that have their cell wall removed mechanically or enzymatically. In most plant species, plant regeneration from protoplasts is challenging and, furthermore, the treatment of the protoplasts with chemical and physical substances influences their viability and capability (Fu et al., 2012). Thus, the development of efficient and cost-effective methods for gene delivery to plant cells is very important.

* Correspondence: nzare@uma.ac.ir

Advances in materials science have led to the design and production of nanoscale materials that could eliminate many barriers and limitations in this respect and may facilitate gene delivery to plant cells. Polyamidoamine (PAMAM) dendrimers are cationic nanostructures that are synthesized stepwise by the addition of spherical layers of methyl acrylate, followed by amidation, around the core molecule (ethylenediamine or ammonia). PAMAM dendrimers have unique molecular properties such as defined architecture, highly branched spherical structures, and low polydispersity that make them attractive materials for gene delivery (Dufès et al., 2005). The number of layers or generations determines the size of the dendrimers. Each additional generation of PAMAM dendrimers leads to the doubling of the amine groups and 10 Å of enlargement in the molecule size (Bielinska et al., 1997). The PAMAM dendrimers interact with nucleic acids through the electrostatic bonds between the negatively charged groups (phosphate) of DNA or RNA and the positively charged groups (amine) on the dendrimers surface, resulting in the formation of dendriplexes. The formation of dendriplexes (dendrimer–DNA complex) leads to a DNA condensation similar to the condensation of the DNA by histones in the chromosomes (Yu and Larson, 2014). In addition, the dendrimers protect the DNA from degradation by cellular nucleases activity (Navarro and de ILarduya, 2009; Wang et al., 2011).

The ability of PAMAM dendrimers to mediate nucleic acid transfer into a wide range of animal cell lines has been reported (Kesharwani et al., 2015; Urbiola et al., 2015; Xiao et al., 2015). However, there are only a few studies on the potential capability of the dendrimers for gene delivery to plant cells (Pasupathy et al., 2008), and the effect of ultrasound on the stability of the PAMAM–DNA complex and the transformation efficiency of plant cells remain unclear. Here, we report the effects of different N/P ratios on hPAMAM (G2)–DNA complex formation and the protection of DNA against degradation by ultrasonic waves and restriction enzymes. In addition, for the first time, this study documents the synergistic effects of ultrasound on the efficiency of PAMAM-mediated gene delivery and expression in intact alfalfa cells.

2. Materials and methods

2.1. Polyamidoamine dendrimers

Hyperbranched PAMAM, generation 2 (hPAMAM-G2), with a diethylenetriamine core and 45 amino groups on the surface was used in this research (Figure 1) (Hemmati et al., 2016).

2.2. Cell culture

Seeds were sterilized with 70% (v/v) ethanol for 30 s and 2% sodium hypochlorite for 15 min and then cultured on MS medium (Murashige and Skoog, 1962). The leaf and petiole explants were prepared from alfalfa (*Medicago sativa* L.) grown in vitro and were cultured on solidified MS medium supplemented with 5 mg/L 2,4-dichlorophenoxyacetic acid (2,4-D) (Duchefa Biochemie, B.V., the Netherlands) and 1 mg/L kinetin (Duchefa Biochemie, B.V.). Friable calli (1–1.5 g) were then transferred to 50 mL of the same medium without agar and maintained at 24 ± 2 °C on a rotary shaker at 120 rpm under 16-h photoperiods and were subcultured every 14 days.

2.3. Construction of the recombinant pUC18 plasmid containing the *gus*A gene (pUC-Gus)

A recombinant pUC18 vector containing the *gus*A gene under control of the cauliflower mosaic virus (CaMV) 35S RNA promoter and nopaline synthase (NOS) terminator was constructed. In brief, pUC18 and pBI121 plasmids were digested with *Hind*III and *Eco*RI restriction enzymes (Thermo Fisher Scientific Inc., Waltham, MA, USA). DNA fragments containing the *gus*A gene cassette (35S promoter-gusA gene-NOS terminator) and also a puc18 plasmid backbone were recovered from the agarose gel using the GF-1 Gel DNA Recovery Kit (Vivantis, Malaysia). The *gus*A gene cassette from pBI121 was then ligated into the pUC18 plasmid using T4 DNA ligase (Invitrogen, USA). The ligation products were introduced into the DH5α strain of *E. coli* through the freeze-and-thaw method (Sambrook and Russell, 2001). The constructed recombinant pUC-*gus*A vector was confirmed by the digestion with the restriction enzymes.

2.4. Preparation of hPAMAM–DNA complex

One milligram of hPAMAM dendrimers (G2) was dissolved in 1 mL of phosphate-buffered saline (pH 7.4) and sonicated for 5 min. The hPAMAM–DNA complex was prepared by the combination of 5 µg of pUC-gusA DNA and PAMAM dendrimers at N/P ratios of 0.25, 0.5, 1, 2, 3, 4, 5, 10, and 20, followed by vigorous vortexing for 30 s and 20 min of incubation at room temperature. The N/P ratios were calculated as the ratio of the amine groups of hPAMAM to the negatively charged phosphate groups in the DNA.

2.5. Ultrasound protection assay

In order to investigate whether hPAMAM dendrimers can protect the plasmid DNA from ultrasound degradation, about 30 µL of the hPAMAM–pDNA complex at different N/P ratios (0, 0.1, 0.2, 0.4, 0.6, 0.8, 1, and 2) was sonicated in an ultrasonic bath with 35 kHz frequency and 160–640 W (Sonorex Digitec, Bandelin, Germany) for 20 s at 25 °C. Then the dendriplex was disassembled according to the methods of Navarro and de ILarduya (2009) and the samples were analyzed by 0.8% agarose gel electrophoresis. Electrophoresis was performed in a 0.8% agarose gel at a constant voltage of 80 V for 60 min in 1X TAE buffer.

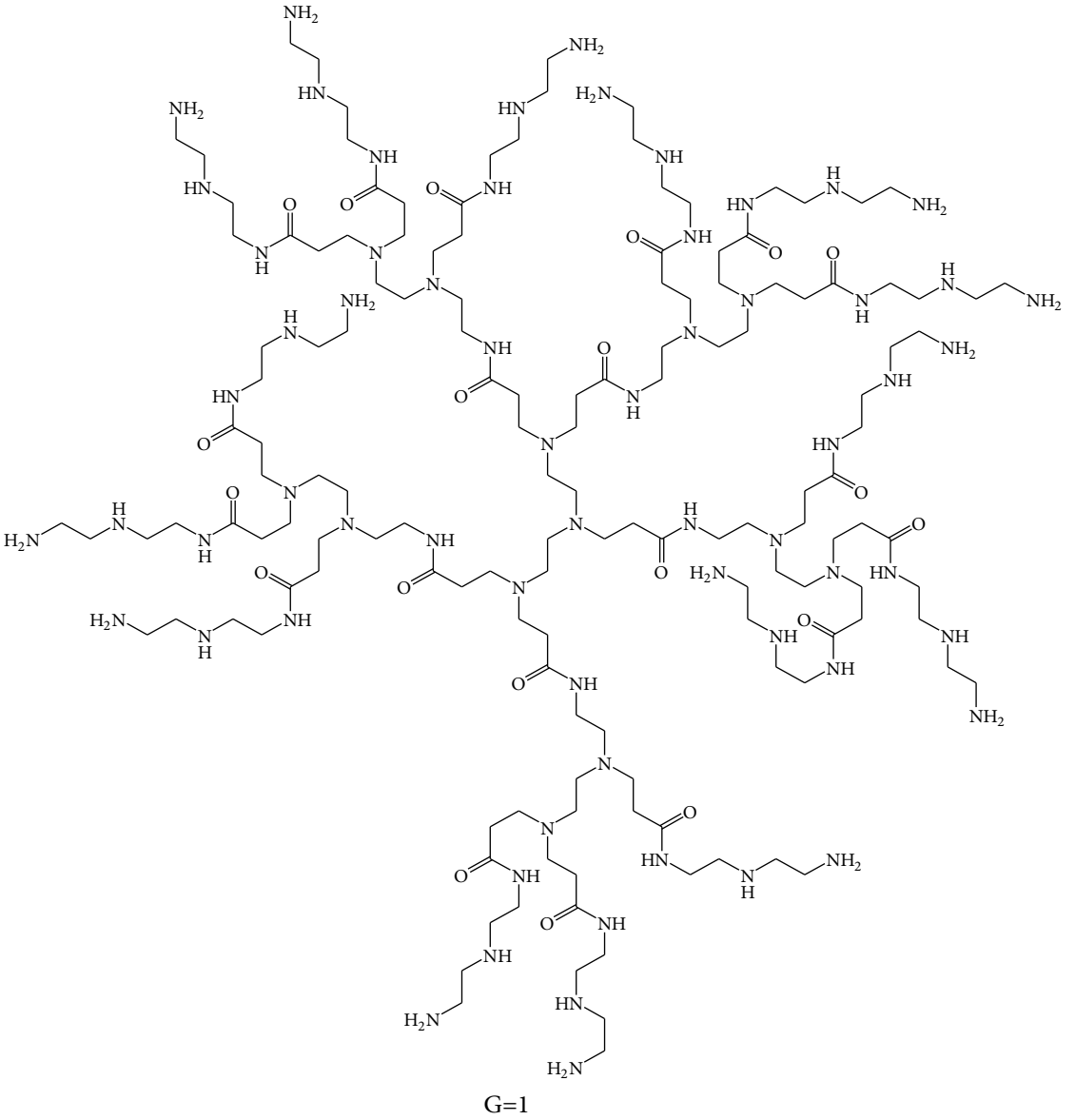

Figure 1. Schematic structure of hPAMAM dendrimers G1 with diethylenetriamine core.

2.6. Restriction enzyme protection assay

In order to assess the effect of hPAMAM–DNA complex formation on pDNA digestion by the restriction enzymes, 200 µL of hPAMAM–DNA complex at N/P ratios of 10, 20, 30, 40, and 50 at a final pDNA concentration of 50 µg/mL was double-digested with *Eco*RI and *Hind*III enzymes at 37 °C for 2 h. Then the enzymes were inactivated and the dendriplex was disassembled according to Navarro and ILarduya (2009). After ethanol precipitation of the DNA and drying at room temperature, the DNA was dissolved in 20 µL of distilled water and then analyzed by 0.8% agarose gel electrophoresis.

2.7. Particle size, zeta-potential, and morphology measurements

To determine the morphology of hPAMAM–DNA complexes, the complexes were prepared at the N/P ratio of 10 in 150 mM NaCl and sonicated for 10 min on ice. The samples were coated with gold/palladium and scanned by LEO 1430VP scanning electron microscope (SEM) using an accelerating voltage of 15 kV. Moreover, dynamic light scattering and zeta-potential analysis were performed to determine the particle sizes and zeta-potential of hPAMAM–DNA complexes using a Malvern Zetasizer (Malvern Instruments, Westborough, MA, USA).

2.8. Cell treatment with ultrasound

In order to obtain the optimum exposure duration for gene delivery to the alfalfa cells treated with ultrasonic waves, the effects of different durations of ultrasound exposure on viability and cell wall damage were examined. The cell suspension cultures of alfalfa were sonicated for 2, 10, and 20 min at 25 °C using an ultrasonic bath (160–640 W, 35 kHz, Sonorex Digitec, Bandelin, Germany). Then the cells were stained using 0.4% Trypan blue (Louis and Siegel, 2011) and the percentage of viable (unstained) cells was determined under light microscopy using a hemocytometer slide.

2.9. Cytotoxicity assay

The cytotoxicity of hPAMAM dendrimers for the alfalfa cells was measured by Trypan blue staining assay. Different concentrations (1, 10, and 50 µg/mL) of hPAMAM were added to 1 mL of the cell suspension with a density of 5 × 10^4 cells/mL and incubated for 6, 24, and 72 h. Then the cells were stained with 0.4% Trypan blue solution and the percentage of viable cells was determined under light microscopy using a hemocytometer slide.

2.10. Ultrasound-assisted PAMAM dendrimers' gene delivery to alfalfa cells

The ability of hPAMAM dendrimers (G2) to transform the alfalfa cells was examined in two separate experiments. In the first experiment, 1 mL of cell suspension culture (5 × 10^5 cells/mL) was incubated for 30 min in MS medium containing 21% sucrose, 5 mg/L 2,4-D, and 1 mg/L kinetin. Then the supernatant was discarded and 0.5 mL of ssDNA-FITC-hPAMAM complex (N/P = 5) or ssDNA-FITC (Bioneer, Daejeon, Korea) was added to the alfalfa cells and then sonicated in an ultrasonic bath (Sonorex Digitec, Bandelin, Germany) with 35 kHz frequency and 160–640 W for 0 and 2 min. Thereafter, cells incubated in the MS medium containing 5 mg/L 2,4-D and 1 mg/L kinetin were maintained at 25 °C on a shaker at 120 rpm for 7 h. The cells were removed from the solution, washed three times with the MS medium, and then observed with a fluorescence microscope (Hund, Germany).

In the second experiment, the ability of the PAMAM dendrimers to deliver plasmid DNA containing the *gus*A reporter gene into the alfalfa cells and the factors affecting the transfection efficiency were examined. For this, 0.5 mL of hPAMAM–DNA (double-strand pUC-gusA plasmid DNA) complex at N/P ratios of 0, 1, 3, 5, 10, and 20 (with a fixed concentration of 5 µg DNA) was mixed with 1 mL of alfalfa cell suspension culture and sonicated for 0, 30, 60, 120, and 180 s. The cells were maintained in the above-mentioned conditions for 72 h. Then the transfection and expression of the *gus*A gene were assessed by the histological GUS assay method (Jefferson, 1987).

2.11. Statistical analysis

All data were analyzed by one-way ANOVA followed by Duncan's multiple range test or least significant difference mean comparisons. All analyses were performed with SPSS 16 (SPSS Inc., Chicago, IL, USA) and SAS Ver. 9 (SAS Institute, Cary, NC, USA) and the graphs were produced using Microsoft Office Excel 2010. All values were presented as mean ± SE.

3. Results

3.1. Construction of recombinant pUC plasmid containing *gus*A gene (pUC-*gus*A)

According to the plasmid map (Figures 2a), it was expected that the restriction of the recombinant plasmid by the *Eco*RI enzyme would result in a fragment 5669 bp long. The band patterns on the agarose gel were consistent with the expected ones (Figure 2b).

3.2. Formation of hPAMAM–DNA complexes

The binding of hPAMAM dendrimers to the plasmid DNA and the complex formation were evaluated by the retardation of DNA migration during agarose gel electrophoresis. As shown in Figure 3a, the electrophoresis of the naked pDNA (lane 1) led to three bands corresponding to open circular, linear, and supercoiled forms of the plasmid. Significant electrophoresis retardation of the plasmid DNA occurred at N/P ratios of 3 and above. The pDNA was completely immobilized by hPAMAM dendrimers at N/P = 4. With increasing N/P ratios, the negative charge of pDNA reduced gradually and continued until complete neutralization at N/P ratios of 4 and above (Figure 3a).

3.3. Stability of the complex against restriction enzyme digestion

To investigate the susceptibility of hPAMAM–DNA complexes to the restriction endonucleases, naked and complexed pDNA (dendriplexes) were incubated with *Eco*RI and *Hind*III enzymes. As shown in Figure 3b, the electrophoretic analysis of DNA dissociated from hPAMAM–DNA complexes indicated that the naked plasmid DNA was completely digested into two expected fragments. In contrast, the plasmid DNA complexed with hPAMAM dendrimers at different N/P ratios was protected from digestion and revealed three bands corresponding to the open circular, linear, and supercoiled forms of the plasmid, similar to untreated (uncut) plasmid DNA (Figure 3b).

3.4. DNA protection from ultrasound damage by hPAMAM dendrimers

The electrophoretic analysis of the dissociated DNA showed that the naked plasmid DNA was severely damaged by ultrasound and appeared as a smear on the agarose gel. However, the DNA that dissociated from hPAMAM–DNA complexes at N/P of 2 remained completely

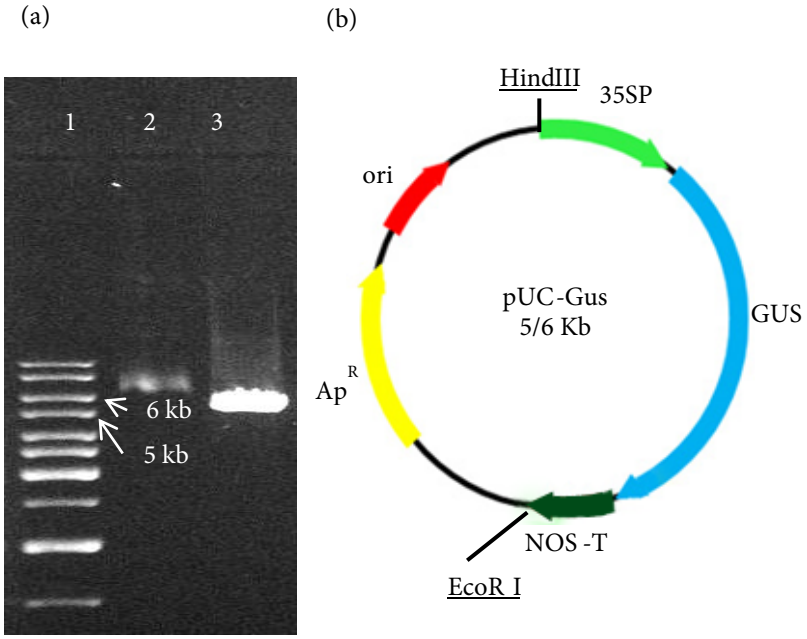

Figure 2. The structure of pUC-gusA vector: (a) pUC-gusA recombinant vector digested with *EcoR*I, lane 1: 1-kb ladder, lane 2: uncut pUC-gusA recombinant vector, lane 3: pUC-gusA plasmid digested with *EcoR*I. (b) The schematic representation of pUC-gusA vector carrying *gus*A gene under control of the CaMV 35S promoter and NOS terminator.

unchanged and showed three bands on the gel, similar to the untreated plasmid DNA (Figure 3c). As shown in Figure 3c, partial protection of the DNA from damage is observed at N/P ratios lower than 2, and with increasing N/P ratios, there is increased protection of the DNA. These results demonstrate that all forms of plasmid DNA in the hPAMAM–DNA complex structure are protected from ultrasound damage, but the degree of protection depends on the N/P ratio.

3.5. Characterization of hPAMAM–DNA complexes

Figure 3d shows the SEM image of the dendriplexes prepared with G2 hPAMAM at an N/P ratio of 10. As shown in Figure 3d, the dendriplexes were individual, spherical, or elliptical, and homogeneously distributed without collapsed complexes. As shown in the Table, particle size and zeta-potential of hPAMAM–DNA complexes were influenced by N/P ratios. The zeta-potential of hPAMAM–DNA complexes at N/P ratio of 1 was –11.00 mV and this became increasingly positive with increases in the N/P ratio from 1 to 10, thereafter staying relatively constant. For example, increasing the N/P ratio from 1 to 10 increased the zeta-potential of hPAMAM–DNA complexes from –11.00 mV to +20 mV, whereas the zeta-potential of complexes at N/P ratio of 20 was +19.3 mV (Table).

Although the particle size of the hPAMAM–DNA complexes at N/P ratios of l and 3 did not significantly change, the particle size of hPAMAM–DNA complexes was also dependent on the N/P ratios; the particle size decreased with increasing N/P ratio from 1 to 10 and increased thereafter. For instance, the size of the complex decreased from 233 ± 14.6 to 176 ± 27.5 and 123 ± 21.3 nm for N/P ratios of 1, 5, and 10, respectively. In contrast, the size of the complex increased to 162.0 with increasing N/P ratio from 10 to 20 (Table). Moreover the largest hPAMAM–DNA complex (238 ± 10.3) was observed at the N/P ratio of 3, which could be due to the lower condensation capacity of this ratio of hPAMAM–DNA compared with higher ratio of hPAMAM–DNA complexes.

3.6. Effect of hPAMAM dendrimers on the viability of alfalfa cells

The effects of different concentrations and exposure times of hPAMAM dendrimers on alfalfa cells were examined by Trypan blue staining. The variance analysis of the cells' viability indicated that the viability of an alfalfa cell was significantly affected by hPAMAM concentration, exposure time, and their interaction. As shown in Figure 4a, hPAMAM dendrimers displayed a concentration- and exposure duration-dependent cytotoxicity, such that with increasing hPAMAM concentration and exposure time, the cell viability was decreased significantly. At 50 µg/mL concentration, the cell viability was 78.30% at 6 h after the treatment, and it decreased to 13.13% and 2.65% at 24 h and 72 h after treatment, respectively. At 10 µg/mL concentration of hPAMAM, alfalfa cell viability

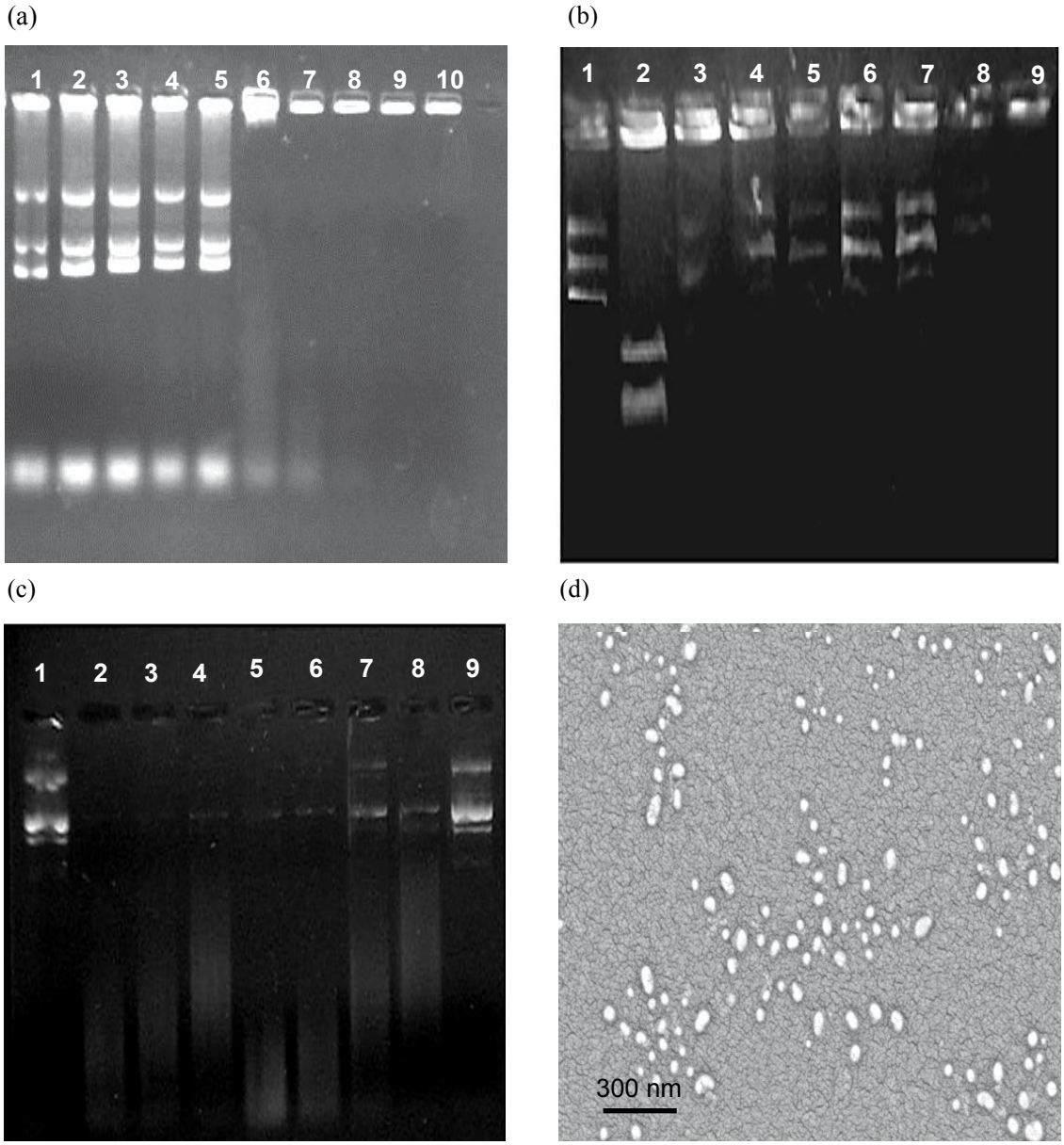

Figure 3. Characteristics of hPAMAM–DNA complexes: (a) DNA mobility retardation assay of hPAMAM–DNA complexes at different N/P ratios, lane 1: N/P ratio of 0 (pDNA only), lanes 2–10: N/P ratios of 0.25, 0.5, 1, 2, 3, 4, 5, 10, and 20, respectively. (b) pDNA protection from endonuclease activity, pDNA dissociated from undigested (lane 1) and digested hPAMAM–DNA complex at N/P ratios of 0, 10, 20, 30, 40, and 50 (lanes 2–7, respectively). (c) pDNA protection from ultrasound damage: pDNA dissociated from nonsonicated (lane 1) and sonicated hPAMAM–DNA complex at N/P ratios of 0, 0.1, 0.2, 0.4, 0.6, 0.8, 1, and 2 (lanes 2–9, respectively). (d) SEM micrograph of G2 hPAMAM–DNA complex at N/P ratio of 10.

was 81.21%, 64.36%, and 11.69% after 6, 24, and 72 h of treatment, respectively.

3.7. Effect of ultrasound on the viability and morphology of alfalfa cells

Analysis of variance indicated that cell viability was significantly ($P < 0.05$) affected by the duration of ultrasound exposure and the percentage of viable cells was decreased with increase in the duration of ultrasound exposure (Figure 4b). As shown in Figure 4b, 76.45% of the cells were viable after 2 min of ultrasound exposure, which reduced to 62.31% after 10 min of exposure. However, a sharp decline in cell viability occurred after 20 min of ultrasound exposure and the percentage of viability was decreased to less than 20.83%.

Light microscopy and SEM analysis of the alfalfa cells indicated that the changes caused by the ultrasound waves

Table. Particle size and surface charge of hPAMAM–DNA complexes prepared at various N/P ratios.

Charge ratios (N/P)	Size		Zeta-potential (mV)
	Z-average (nm)	PDI	
1	233 ± 14.6	0.340	–11 ± 4.64
3	238 ± 10.3	0.384	–1.94 ± 5.17
5	176 ± 27.5	0.027	6.25 ± 6.01
10	123 ± 21.3	0.027	20.9 ± 5.57
20	162 ± 24.7	0.034	19.3 ± 7.56

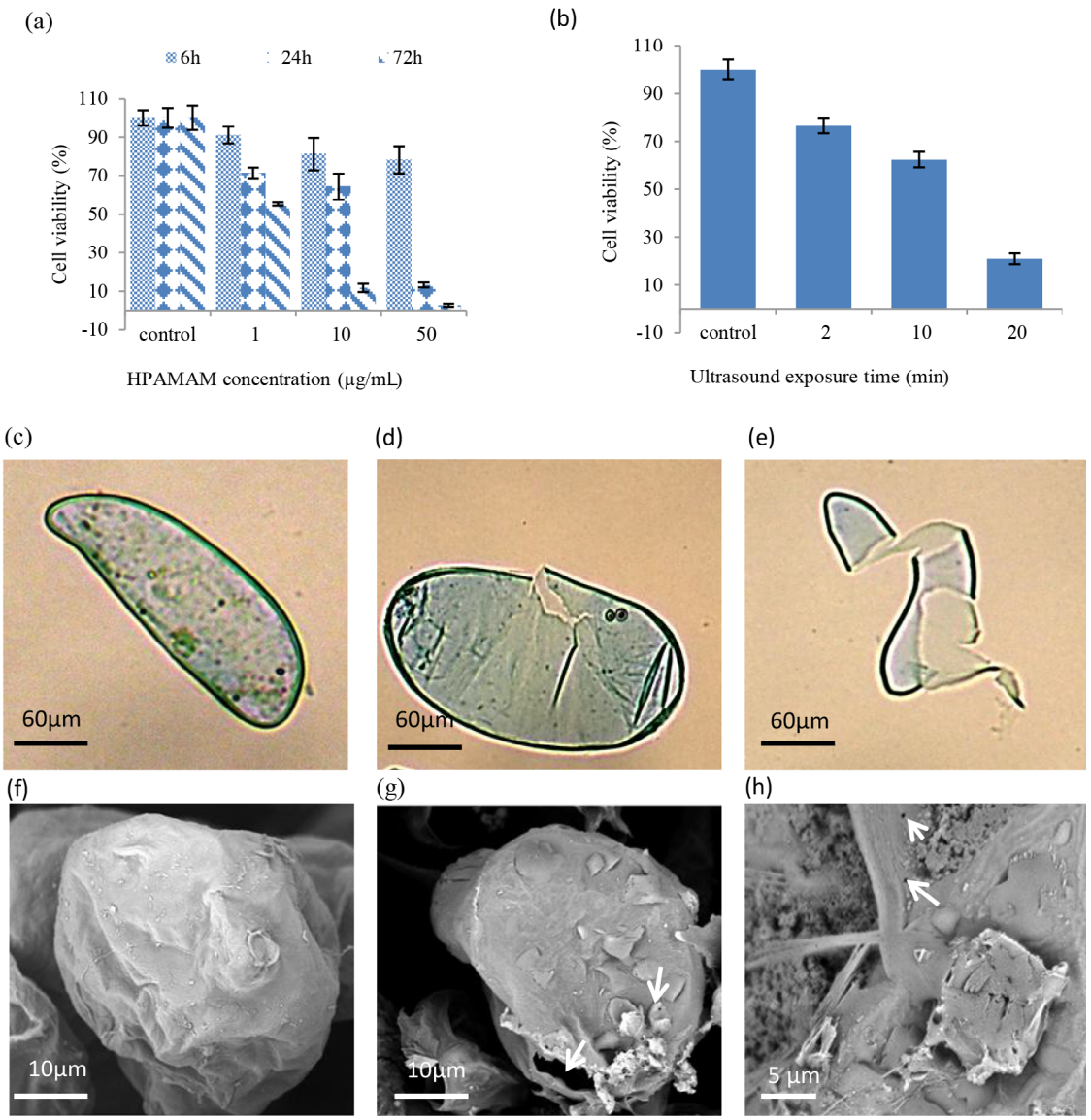

Figure 4. (a) The alfalfa cells' viability under the effect of different concentrations and exposure durations of G2 hPAMAM; (b) the effect of different exposure durations of ultrasound on the alfalfa cells' viability. The control (c) and sonicated (d and e) alfalfa cells were observed by light microscopy. The control cells (f) and changes caused by sonication (g and h) in alfalfa cells were analyzed by SEM.

varied from holes and small gaps to a complete collapse of the cells (Figures 4c–4h). Therefore, 30–180 s of ultrasound exposure could be used to enhance the efficiency of gene delivery to alfalfa cells by using nanoparticles.

3.8. Transfection of alfalfa cells with hPAMAM-ssDNA-FITC

We studied the effects of ultrasound and hPAMAM on ssDNA-FITC delivery into the alfalfa cells. The alfalfa control cells and cells treated with ssDNA-FITC alone did not show any fluorescence emissions (Figures 5a–5d), whereas 1.4% of the cells treated with ssDNA-FITC and ultrasound showed fluorescent emission (Figures 5e and 5f). However, 36% of the alfalfa cells treated with hPAMAM-ssDNA-FITC and ultrasound (for 2 min) showed fluorescent emission, indicating that the combination of PAMAM dendrimers and ultrasound can effectively improve the efficiency of DNA delivery into intact alfalfa cells (Figures 5g and 5h). These results demonstrated that ssDNA-FITC was incapable of penetrating alfalfa cell walls without hPAMAM dendrimers or ultrasound (Figure 5i).

3.9. Gene transfer into alfalfa cells with G2 hPAMAM

The effects of different N/P ratios and ultrasound durations on the transfection efficiency (percentage of GUS-expressing cells or GUS-positive cells) were examined by GUS histochemical assay (Figures 6a–6c). Analysis of variance for the percentage of GUS-positive cells revealed that the transfection efficiency was significantly influenced by the N/P ratio and duration of ultrasound

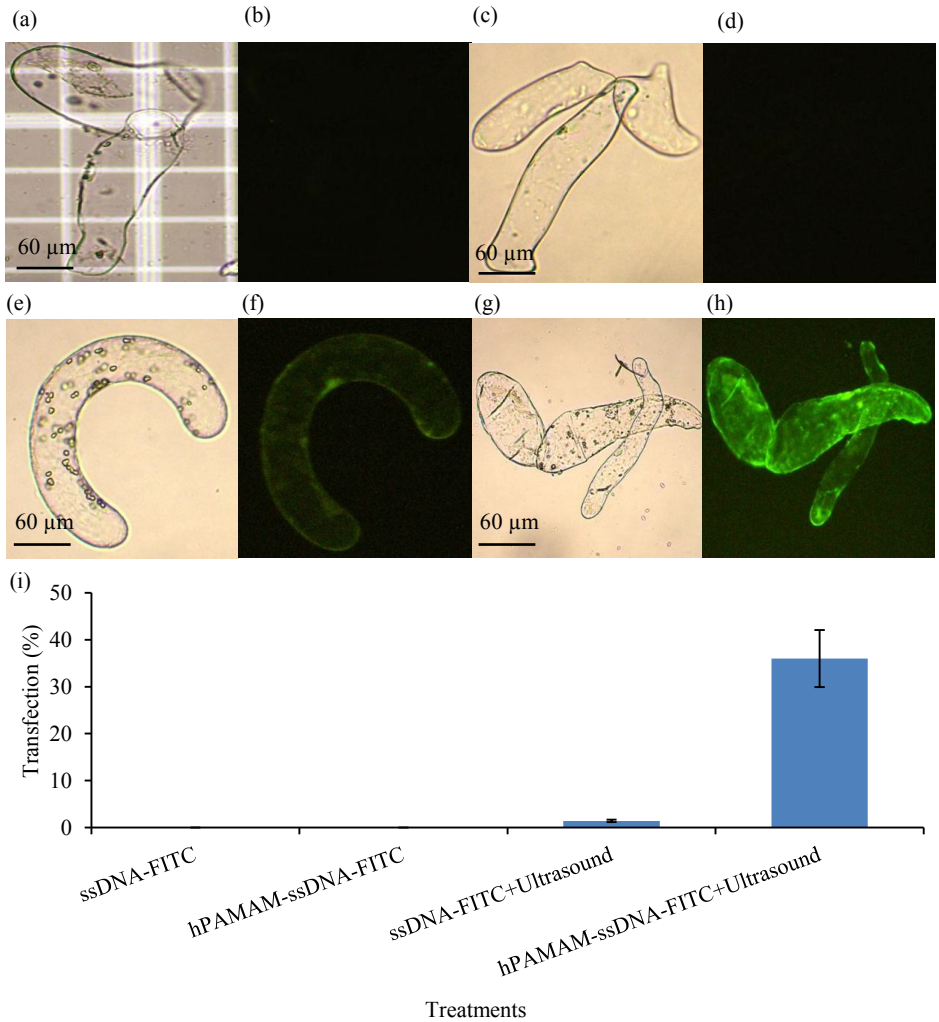

Figure 5. Fluorescence microscopy analysis of the alfalfa cells. Bright-field (a) and fluorescence (b) images of the untreated (control) alfalfa cells. Bright-field (c) and fluorescence (d) images of the alfalfa cells incubated with ssDNA-FITC. Bright-field (e) and fluorescence (f) images of the alfalfa cells incubated with ssDNA-FITC and ultrasound. Bright-field (g) and fluorescence (h) images of the alfalfa cells incubated with hPAMAM-ssDNA-FITC and ultrasound. (i) Effects of hPAMAM dendrimers and ultrasound on the transfection of the alfalfa cells with ssDNA-FITC.

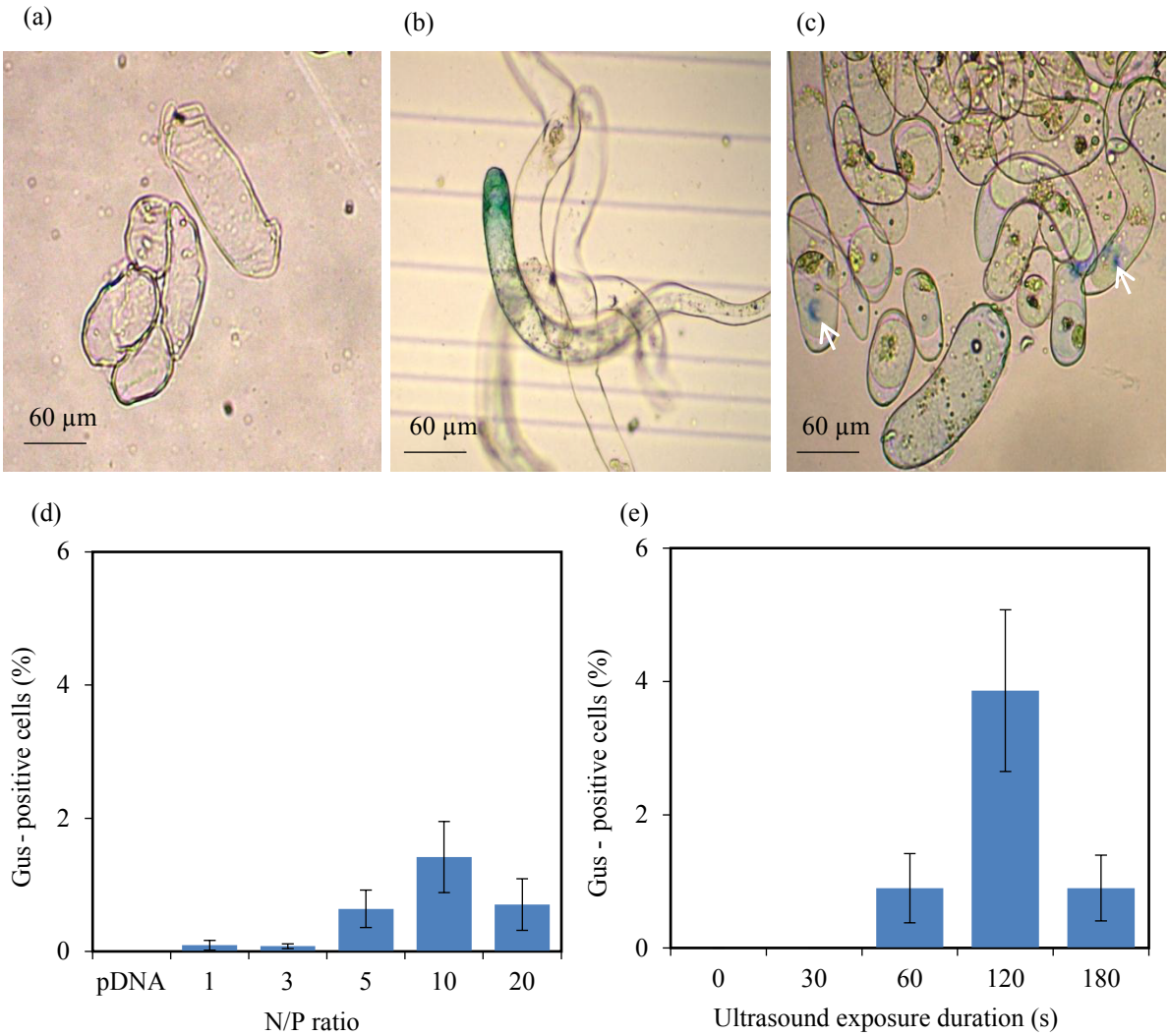

Figure 6. GUS histochemical assay. (a) Untreated (control) alfalfa cells and (b and c) the alfalfa cells transfected by hPAMAM–DNA complexes. The effects of different N/P ratios (d) and different durations of ultrasound exposure (e) on the efficiency of alfalfa cell transfection by hPAMAM–DNA complexes.

exposure, whereas the interaction between N/P ratio and ultrasound duration was not statistically significant at the 5% level of probability. As shown in Figure 6d, transfection and *gus*A gene expression efficiency increased with increase in the N/P ratio until transfection and expression efficiency reached 1.42% at the N/P ratio of 10, which was significantly higher than that of the control (pDNA). Beyond this optimum N/P ratio, the transfection and expression efficiency started to decrease.

The alfalfa cells showed a time-dependent transfection response to ultrasound. The utilization of hPAMAM–DNA complexes at the N/P ratio of 10 revealed that increased ultrasound exposure duration resulted in higher transfection efficiency until it reached 3.86% at 120 s of sonication. Thereafter, the percentage of GUS-positive cells decreased rapidly (Figure 6e). This reduction could be attributed to degrading the hPAMAM–DNA complexes by ultrasound at higher exposure durations.

4. Discussion

In recent years, the utilization of nanoparticles in plant biology has been considered because of advantages such as their capability for interaction with DNA and its protection against mechanical and enzymatic shearing (Bande et al., 2015), and also macromolecules' transfer into intact plant cells (Pasupathy et al., 2008; Liu et al., 2009; Naqvi et al., 2012). Dendrimers with different generations and surface groups have been synthesized, characterized, and tested in a wide range of animal cells (Mallick and Choi, 2015; Urbiola et al., 2015). However, there are few reports on the utilization of dendrimers as gene delivery carriers for plant cells (Pasupathy et al., 2008). The interaction of DNA with

dendrimers (dendriplex formation) and its condensation by the dendrimers depends on several factors, such as the N/P (charge) ratio and the dendrimers' generation (Lee and Larson, 2006; Yu and Larson, 2014). It has been reported that the smaller G2 PAMAMs, due to their more fluid structure, could bind to DNA better than the larger G6 PAMAMs (Kabanov et al., 2000).

Dendrimer–DNA binding and complex formation could be determined by the retardation in DNA mobility during agarose gel electrophoresis (Sarkar et al., 2013). As shown in Figure 3a, the retardation analysis indicated the formation of dendriplexes through charged complex formation (charge interactions) between hPAMAM and DNA. On the other hand, the cationic amine groups on the PAMAM dendrimers bind to the negatively charged DNA via electrostatic interactions and neutralize the DNA completely at N/P ratios of 4 and above.

Most of the naked DNA delivered into the cells undergoes rapid degradation by the defense mechanisms of the cells (Howell et al., 2003; Al-Dosari and Gao, 2009). Plasmid DNA complexed with hPAMAM at N/P ratios higher than 10 was protected completely from digestion by the restriction enzymes (Figure 3b), but at N/P ratios lower than 10, the protection of DNA was less complete. It seems that at N/P ratios lower than 10, the DNA is not completely covered by hPAMAM and, therefore, the enzyme could bind to DNA and cut it. Therefore, at N/P ratios higher than 10, the complex formation of DNA with hPAMAM reduces the accessibility of the DNA to nucleases. This reduced accessibility of the complexed DNA to enzymes can prolong its survival in the cell and increase the duration of transient gene expression and also its genomic integration. However, it should be mentioned that resistance of the complexed DNA to restriction enzymes could be higher than its resistance to the cellular nuclease activity (Abdelhady et al., 2013; Dehshahri et al., 2013).

It has been shown that low intensity levels of ultrasound cause various nonlethal mechanical and biological effects on the cells and have potential uses in plant biotechnology and genetic engineering (Liu et al., 2006). Sonication-mediated DNA delivery into protoplasts and intact plant cells have been reported in different plants and possess benefits such as lower costs, being species-independent, and simplicity (Joersbo and Brunstedt, 1990; Zhang et al., 1991; Choudhary and Chin, 1995). However, naked DNA is sensitive to ultrasound damage and is rapidly fragmented during the sonication process (Figure 3c). DNA degradation under ultrasound treatment occurs mainly through destroying the hydrogen bonds and by breaking the phosphodiester bonds in single and double strands of the DNA helix (Grokhovsky et al., 2011). As shown in Figure 3c, hPAMAM dendrimers effectively protected the DNA from ultrasonic degradation, so hPAMAM–DNA complexes effectively protected the DNA from ultrasonic degradation and allowed the simultaneous utilization of the advantages of both nanoparticle- and ultrasound-mediated gene delivery systems.

The morphology of nanoparticles plays a key role in transfection efficiency (Venkataraman et al., 2011). As shown in Figure 3d, SEM analysis revealed that hPAMAM–DNA complexes have rounded and spherical shape. Previous studies showed that spherical nanoparticles have higher transfection efficiency than other shapes of nanoparticles (Jiang et al., 2013). As shown in the Table, there is a clear correlation between N/P ratio and complex size. The size evaluation of hPAMAM–DNA complexes reveals that the smallest particle size was obtained at N/P ratio of 10. This could be due to the higher condensation capacity at this N/P ratio. Furthermore, the hPAMAM–DNA complexes were uniform in size at N/P ratios above 3, as shown by the low polydispersity index (PDI) (Table). However, the sizes of complexes were increased at N/P of 20 as compared to the N/P ratio of 10. This could be due to the extra aggregation of hPAMAM around hPAMAM–DNA complexes (Gary et al., 2013).

It has been reported that the size of complexes derived from the interaction of DNA and polycations such as PAMAM dendrimer, poly (L-lysine), and polyethylenimine depends on the size and topology of the DNA and will be reduced with a decrease in the size of the DNA molecules (Hsu and Uludağ, 2008; Yu et al., 2013).

The cationic charge of the polymer is one of the most important factors for DNA condensation and gene delivery into eukaryotic cells. Cationic polymers such as PAMAM interact with the cells through electrostatic interactions between the cationic groups on PAMAM dendrimers and the anionic surface of the cells (Perico, 2016), which may be important for the cellular uptake of DNA complexed with PAMAM. Regarding the zeta-potential results, increasing the N/P ratio from 1 to 10 appeared to significantly increase the surface charge of hPAMAM–DNA complexes. On the other hand, interactions between positively charged amines on the hPAMAM surface and negatively charged groups on the DNA backbone cause an increasingly positive charge in the PAMAM–DNA complexes (Mou et al., 2016). However, there were no significant differences in the surface charge of hPAMAM–DNA complexes at N/P ratios of 10 and 20. This may be due to the fact that the DNA was completely saturated with hPAMAM at the N/P ratio of 10.

These interactions could destabilize the cell membrane (Dufès et al., 2005) and result in cytotoxicity and cell lysis. The generation of PAMAM dendrimers and therefore the number of terminal amino groups are critical determinants in cytotoxicity. Generally, higher generations of PAMAMs cause more cytotoxicity (Pryor et al., 2014). The alfalfa

cells showed a concentration- and exposure duration-dependent response to G2 hPAMAM. At 1, 10, and 50 µg/mL concentrations of hPAMAM, no significant decrease in cell viability was observed until 6 h after treatment. At 10 µg/mL concentration, the significant part of alfalfa cell death occurred between 24 and 72 h, and about 88% of the cells lost their viability at 72 h after the treatment. However, at 50 µg/mL concentration, the obvious cell death happened between 6 h and 24 h and about 87% of the cells had lost their viability 24 h after the treatment (Figure 4a).

Here, we demonstrate the synergistic effects of ultrasound and hPAMAM dendrimers on alfalfa cell transfection. As shown in Figures 5 and 6, no transfected cells were obtained by the treatment of the alfalfa cells with ssDNA-FITC and also with plasmid DNA, indicating that the inability of the naked DNA to pass through cell walls and membranes may be due to the inappropriate morphology, size, and charge (Al-Dosari and Gao, 2009). The sonication of the alfalfa cells in the presence of ssDNA-FITC resulted in transferring of the labeled DNA into the alfalfa cells with efficiency of 1.4%. In contrast, treatment of the cells with ssDNA-FITC-hPAMAM complexes did not lead to detectable transfected and fluorescent cells. The sonication of the cells in the presence of ssDNA-FITC-hPAMAM complexes increased the transfection efficiency to 36%, which was 25.7-fold that of sonication + ssDNA-FITC (Figure 5i). These results indicate the synergistic effects of hPAMAM dendrimers with ultrasound treatment on the transfection of the alfalfa cells. Similar results were obtained from the transfection of the alfalfa cells with the *gus*A gene. Therefore, as shown in Figure 6e, the highest efficiency of transfection and expression of GUS protein was achieved with the combination of 120 s of ultrasound and hPAMAM–DNA complexes with N/P ratios of 10. However, the transfection efficiency was decreased when the N/P ratio increased to higher than 10 (Figure 6d). This reduction may be due to the saturation of DNA by hPAMAM at the N/P ratio of 10. As a result, at N/P ratios higher than 10, the anionic plant cells were coated with positive free hPAMAM particles and therefore created a physical barrier and limited the cellular uptake of hPAMAM–DNA complexes (Pasupathy et al., 2008).

The transfection of animal cells by cationic polymers typically involves the electrostatic binding of the cationic complex to the anionic groups (e.g., phospholipids and/or glycolipids) of the cell surface, cellular uptake by endocytosis, and, finally, endosomal escape into the cytoplasm (Dufès et al., 2005; Kesharwani et al., 2012). Cavitation-induced wounding is an important biological effect of ultrasound on the cells, forming a large number of repairable micropores on the cell membrane and wall (Liu et al., 2006; Qin et al., 2012). On the other hand, low intensity levels of ultrasound transiently enhance the cell membrane permeability and facilitate the passing in or out of substances through the membrane, which can result in the uptake of DNA molecules as well as the DNA–PAMAM complexes.

Acknowledgment

The authors thank Dr F Najafi of the Institute for Color Science and Technology (ICST) for providing hPAMAM dendrimers.

References

Abdelhady HG, Lin YL, Sun H, ElSayed ME (2013). Visualizing the attack of RNase enzymes on dendriplexes and naked RNA using atomic force microscopy. PLoS One 8: e61710.

Al-Dosari MS, Gao X (2009). Nonviral gene delivery: principle, limitations, and recent progress. AAPS J 11: 671-681.

Altpeter F, Baisakh N, Beachy R, Bock R, Capell T, Christou P, Daniell H, Datta K, Datta S, Dix PJ et al. (2005). Particle bombardment and the genetic enhancement of crops: myths and realities. Mol Breeding 15: 305-327.

Bande F, Arshad SS, Bejo MH, Kamba SA, Omar AR (2015). Synthesis and characterization of chitosan-saponin nanoparticle for application in plasmid DNA delivery. J Nanomater 16: 207.

Bielinska AU, Kukowska-Latallo JF, Baker JR (1997). The interaction of plasmid DNA with polyamidoamine dendrimers: mechanism of complex formation and analysis of alterations induced in nuclease sensitivity and transcriptional activity of the complexed DNA. Biochim Biophys Acta 1353: 180-190.

Burris KP, Dlugosz EM, Collins AG, Stewart CN Jr, Lenaghan SC (2016). Development of a rapid, low-cost protoplast transfection system for switchgrass (*Panicum virgatum L.*). Plant Cell Rep 35: 693-704.

Choudhary M, Chin CK (1995). Ultrasound mediated delivery of compounds into petunia protoplasts and cells. J Plant Biochem Biotech 4: 37-39.

Daniell H, Vivekananda J, Nielsen B, Ye G, Tewari K, Sanford J (1990). Transient foreign gene expression in chloroplasts of cultured tobacco cells after biolistic delivery of chloroplast vectors. P Natl Acad Sci USA 87: 88-92.

Dehshahri A, Alhashemi SH, Jamshidzadeh A, Sabahi Z, Samani SM, Sadeghpour H, Mohazabieh E, Fadaei M (2013). Comparison of the effectiveness of polyethylenimine, polyamidoamine and chitosan in transferring plasmid encoding interleukin-12 gene into hepatocytes. Macromol Res 21: 1322-1330.

Dufès C, Uchegbu IF, Schätzlein AG (2005). Dendrimers in gene delivery. Adv Drug Deliv Rev 57: 2177-2202.

Finer JJ, Vain P, Jones MW, McMullen MD (1992). Development of the particle inflow gun for DNA delivery to plant cells. Plant Cell Rep 11: 323-328.

Frame BR, Drayton PR, Bagnall SV, Lewnau CJ, Bullock WP, Wilson HM, Dunwell JM, Thompson JA, Wang K (1994). Production of fertile transgenic maize plants by silicon carbide whisker-mediated transformation. Plant J 6: 941-948.

Farsani MK, Amraie E, Kavian P, Keshvari M (2016). Effects of aqueous extract of alfalfa on hyperglycemia and dyslipidemia in alloxan-induced diabetic Wistar rats. Interv Med Appl Sci 3: 103-108.

Fu YQ, Li LH, Wang PW, Qu J, Fu YP, Wang H, Sun JR, Lv CL (2012). Delivering DNA into plant cell by gene carriers of ZnS nanoparticles. Chem Res Chinese U 28: 672-676.

Gary DJ, Min J, Kim Y, Park K, Won YY (2013). The effect of N/P ratio on the in vitro and in vivo interaction properties of PEGylated poly[2-(dimethylamino)ethyl methacrylate]-based siRNA complexes. Macromol Biosci 13:1059-1071.

Grokhovsky SL, Il'Icheva IA, Nechipurenko DY, Golovkin MV, Panchenko LA, Polozov RV, Nechipurenko YD (2011). Sequence-specific ultrasonic cleavage of DNA. Biophys J 100: 117-125.

Hemmati M, Kazemi B, Najafi F, Zarebkohan A, Shirkoohi R (2016). Synthesis and evaluation of a glutamic acid-modified hPAMAM complex as a promising versatile gene carrier. J Drug Target 24: 408-421.

Howell DPG, Krieser RJ, Eastman A, Barry MA (2003). Deoxyribonuclease II is a lysosomal barrier to transfection. Mol Ther 8: 957-963.

Hsu CYM, Uludağ H (2008). Effects of size and topology of DNA molecules on intracellular delivery with non-viral gene carriers. BMC Biotechnol 8: 23.

Jefferson RA (1987). Assaying chimeric genes in plants: the GUS gene fusion system. Plant Molec Biol Pep 5: 387-405.

Jiang X, Qu W, Pan D, Ren Y, Williford JM, Cui H, Luijten E, Mao HQ (2013). Plasmid-templated shape control of condensed DNA-block copolymer nanoparticles. Adv Mater 25:227-232.

Joersbo M, Brunstedt J (1990) Direct gene transfer to plant protoplasts by mild sonication. Plant Cell Rep 9: 207-210.

Kabanov V, Sergeyev V, Pyshkina O, Zinchenko A, Zezin A, Joosten J, Brackman J, Yoshikawa K (2000). Interpolyelectrolyte complexes formed by DNA and Astramol poly (propylene imine) dendrimers. Macromolecules 33: 9587-9593.

Kesharwani P, Banerjee S, Gupta U, Amin MCIM, Padhye S, Sarkar FH, Iyer AK (2015). PAMAM dendrimers as promising nanocarriers for RNAi therapeutics. Mater Today 18: 565-572.

Kesharwani P, Gajbhiye V, Jain NK (2012). A review of nanocarriers for the delivery of small interfering RNA. Biomaterials 33: 7138-7150.

Lee H, Larson RG (2006). Molecular dynamics simulations of PAMAM dendrimer-induced pore formation in DPPC bilayers with a coarse-grained model. J Phys Chem B 110: 18204-18211.

Ling HQ, Binding H (1997). Transformation in protoplast cultures of *Linum usitatissimum* and *L. suffruticosum* mediated with PEG and with Agrobacterium tumefaciens. J Plant Physiol 151: 479-488.

Liu Q, Chen B, Wang Q, Shi X, Xiao Z, Lin J, Fang X (2009). Carbon nanotubes as molecular transporters for walled plant cells. Nano Lett 9:1007-1010.

Liu Y, Yang H, Sakanishi A (2006). Ultrasound: mechanical gene transfer into plant cells by sonoporation. Biotechnol Adv 24: 1-16.

Louis KS, Siegel AC (2011). Cell viability analysis using trypan blue: manual and automated methods. In: Stoddart MJ, editor. Mammalian Cell Viability: Methods and Protocols, Vol. 740. Berlin, Germany: Springer, pp. 7-12.

Mallick S, Choi JS (2015). Polyamidoamine (PAMAM) dendrimers modified with short oligopeptides for early endosomal escape and enhanced gene delivery. Int J Pharm 492: 233-243.

Mou Q, Ma Y, Jin X, Zhu X (2016). Designing hyperbranched polymers for gene delivery. Mol Syst Des Eng 1: 25-39.

Murashige T, Skoog F (1962). A revised medium for rapid growth and bio assays with tobacco tissue cultures. Physiol Plant 15: 473-497.

Nanasato Y, Konagaya KI, Okuzaki A, Tsuda M, Tabei Y (2013). Improvement of Agrobacterium-mediated transformation of cucumber (*Cucumis sativus* L.) by combination of vacuum infiltration and co-cultivation on filter paper wicks. Plant Biotechnol Rep 3: 267-276.

Naqvi S, Maitra A, Abdin M, Akmal M, Arora I, Samim M (2012). Calcium phosphate nanoparticle mediated genetic transformation in plants. J Mater Chem 22: 3500-3507.

Navarro G, de ILarduya CT (2009). Activated and non-activated PAMAM dendrimers for gene delivery in vitro and in vivo. Nanomedicine 5: 287-297.

Park SH, Jeong JS, Do Choi Y, Kim JK (2015). Characterization of the rice RbcS3 promoter and its transit peptide for use in chloroplast-targeted expression. Plant Biotechnol Rep 9: 395-403.

Pasupathy K, Lin S, Hu Q, Luo H, Ke PC (2008). Direct plant gene delivery with a poly (amidoamine) dendrimer. Biotechnol J 3: 1078-1082.

Perico A (2016). Electrostatic theory of the assembly of PAMAM dendrimers and DNA. Biopolymers 105: 276-286.

Pryor JB, Harper BJ, Harper SL (2014). Comparative toxicological assessment of PAMAM and thiophosphoryl dendrimers using embryonic zebrafish. Int J Nanomedicine 17: 1947-56.

Qin P, Xu L, Zhong W, Yu AC (2012). Ultrasound-microbubble mediated cavitation of plant cells: effects on morphology and viability. Ultrasound Med Biol 38: 1085-1096.

Sambrook J, Russell DW (2001). Molecular Cloning: A Laboratory Manual. 3rd ed. Cold Spring Harbor, NY, USA: Cold Spring Harbor Laboratory Press.

Sarkar K, Chatterjee A, Chakraborti G, Kundu PP (2013). Blood compatible N-maleyl chitosan-graft-PAMAM copolymer for enhanced gene transfection. Carbohydr Polym 98: 596-606.

Smith SR, Bouton JH, Singh A, McCaughey WP (2000). Development and evaluation of grazing-tolerant alfalfa cultivars: a review. Can J Plant Sci 80: 503-512.

Tohidifar M, Zare N, Jouzani GS, Eftekhari SM (2013). *Agrobacterium*-mediated transformation of alfalfa (*Medicago sativa*) using a synthetic *cry3a* gene to enhance resistance against alfalfa weevil. Plant Cell Tiss Org 113: 227-235.

Urbiola K, Blanco-Fernández L, Navarro G, Rödl W, Wagner E, Ogris M, de Ilarduya CT (2015). Evaluation of improved PAMAM-G5 conjugates for gene delivery targeted to the transferrin receptor. Eur J Pharm Biopharm 94: 116-122.

Venkataraman S, Hedrick JL, Ong ZY, Yang C, Ee PLR, Hammond PT, Yang YY (2011). The effects of polymeric nanostructure shape on drug delivery. Adv Drug Deliv Rev 14: 1228-1246.

Wang H, Shi HB, Yin SK (2011). Polyamidoamine dendrimers as gene delivery carriers in the inner ear: how to improve transfection efficiency (review). Exp Ther Med 2: 777-781.

Xiao S, Castro R, Rodrigues J, Shi X, Tomás H (2015). PAMAM dendrimer/pDNA functionalized-magnetic iron oxide nanoparticles for gene delivery. J Biomed Nanotechnol 11: 1370-1384.

Xiong AS, Peng RH, Zhuang J, Chen JM, Zhang B, Zhang J, Yao QH (2011). A thermostable β-glucuronidase obtained by directed evolution as a reporter gene in transgenic plants. PLoS One 6: e26773.

Yu S, Larson RG (2014). Monte-Carlo simulations of PAMAM dendrimer–DNA interactions. Soft Matter 10: 5325-5336.

Yu S, Li MH, Choi SK, Baker JR, Larson RG (2013). DNA condensation by partially acetylated poly (amido amine) dendrimers: effects of dendrimer charge density on complex formation. Molecules 18: 10707-10720.

Zhang LJ, Cheng LM, Xu N, Zhao NM, Li CG, Yuan J, Jia SR (1991). Efficient transformation of tobacco by ultrasonication. Nature Biotechnol 9: 996-997.